UCLouvain

École polytechnique de Louvain

Parametric Study of Lunar Landers

Author: **Miguel Ángel Cortés de Mingo**
Supervisor: **Paul Fisette**
Readers: **Vincent Legat, Philippe Chatelain**
Academic year 2018–2019
Master [120] in Mechanical Engineering

Contents

1 List of Figures

List of Figures

Abstract

This thesis aims at presenting a first model to quantitatively assess how two configurations of propulsion (thruster cluster and gimbaled thruster) influence the maneuverability of planetary landers, understand limitations and assess the boundary conditions to provide the optimal design solution(s).

As a key exploration destination, the Moon was chosen as a practical test case in conjunction with the geometry and mass properties from the Apollo Lunar Module program. This is only a specific example to study but with the model presented can be easily changed to adapt it to other landers or planetary bodies.

To find useful decision-making information, the dynamics of both configurations performing a soft landing were modelled and tested via numerical simulations. with the multibody software ROBOTRAN [1] and a control implementation in MATLAB. Thanks to the symbolic generation of the equations of motion, ROBOTRAN simulates the model and analyses the problem at hand . Indeed, its modularity gives the user the freedom to model complex articulated systems very easily, while retaining a deep understanding of the problem.

The parameters under study are the mass of the payload and the maximum thrust of the thrusters. The optimization objectives refer to the maximum acceleration (truly important for manned missions), the amount of fuel used to control the spacecraft and the mechanical stresses on the structure and on the actuators.

The numerical results will show the optimal configuration (i.e. thruster cluster or gimbaled) for specified parameter ranges (e.g. for the payload mass). The thesis also discusses how the criteria for a good design may change depending on the application. Thanks to this project, designers will make the most of a faster approach, to quantify how each system dynamically performs and to evaluate its limitations.

The project originates from an initiative of SABCA's actuation system business unit in collaboration with the Mechatronics Division (MEED) of the Université catholique de Louvain.

2 Introduction

2.1 Objectives

One of the key ambitions of space exploration is to land on different planetary bodies. The spacecrafts' modules which perform soft landing (i.e. which doesn't end in the destruction of the payload and/or the vehicle) are denominated Landers. In order to successfully achieve this goal, we have to study the parameters that influence the Lander's design process, to optimize and improve the designs already existent.

In this design process, an important decision is on the propulsion and attitude control systems. The correct choice of these two aspects can save fuel, lower the costs, and lead to a better dynamic performance (e.g. avoiding objects, landing on the right spot...). This thesis aims at presenting a methodology to help future designers in this decision-making process. To do so, we use a multibody dynamics approach, whose versatility makes relatively easy change different parameters to adapt

the model to different geometries or trajectories.

To be more specific, the problem we are going to tackle is the choice between two propulsion configurations (Thruster Cluster and Gimbaled Thruster). The first one bases its control in multiple engines. The second configuration is a main engine which can tilt to orientate the lander with the use of electromechanical or hydraulic actuators. This apparently simple decision is crucial in the fuel consumption as well as the total weight of the lander, which can be translated to costs.

The rising private interest in space and the future perspective of the space exploration (e.g. Blue Origin, Space X...), increases the cost-reduction interest. This study aims at set the optimal configurations to reduce expenses, stresses and risks. At the end we will also discuss, after considering the results, possible applications for each configuration (i.e. manned missions, rovers, sample return missions...).

2.2 Preliminary Research

In this chapter we evaluate the different landers, as well as the most suitable rocket engines existent. This give us a general view of the current and past designs.

2.2.1 Landers

A) Luna programme

The Soviet Union started this program in 1959 and ended in 1976. Twenty four spacecraft were officially given the Luna designation but more were launched. They launched, landers, orbiters, sample return and rover missions. Fifteen of them were successful, some of the achievements of this program were the first human object on the moon, the first soft landing and the first artificial satellite of the Moon. Luna 16,20 and 24 also collected samples of lunar soil.

The Luna 9 performed without legs the first soft landing (It used airbags), and its mass was around 100 Kg. The Luna 24, the most recent one, had four pods and the launch mass was 4,800 Kg.

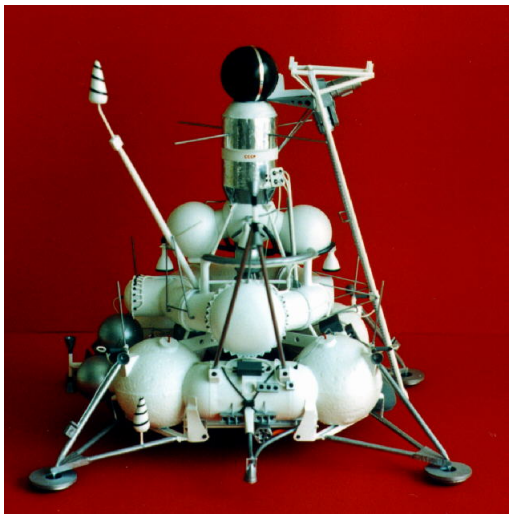

Figure 1: Luna 24 model. Image credit: Phys.org

B) Surveyor

The NASA sent seven spacecrafts to prove the feasibility of soft landing on the moon between 1966 and 1968. They also evaluated the optimal landing area and the thickness of the dust on the surface. They are all on the moon as they were never intended to return. The take off mass was 1000 Kg and landing was about 300 kg. The structure was with only three legs. It had three vernier engines as propulsion plant. This program was a previous step to reach the goal of manned missions.

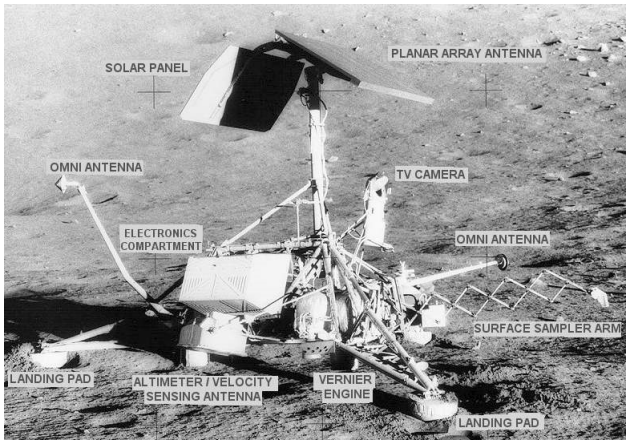

Figure 2: Suveyor on the moon, picture taken during Apollo 12 mission. Source: NASA

Figure 3: Apollo Lunar Lander. Source: NASA

C) Apollo

Program Apollo was the third USA human spacecraft project carried out by the NASA, which accomplished in 1959 the first manned landing on the Moon. This mission was the Apollo 11 and the propulsion system used to land was the Lunar Module Descent Engine, a variable-throttle hypergolic rocket engine developed by Space Technology Laboratories. The lander was automatically controlled by a gimbaled thruster and had also the ability to be directly controlled by the pilots for precise movements.

The main characteristics are summarized in the tables below. (*For further info Appendix A and [1]*)

Lunar Module Descent Engine	
Thrust full throttle	44.037 kN
Minimum Thrust	5.693 kN
Weight	158 Kg
Length	2.413 m
Exit diameter	1.6 m

Lunar Module (Legs extended)	
Height	6.74 m
Diameter	9.45 m
Weight	16374 Kg
Length	2.413 m
Number of legs	4

Table 1: Propulsion and geometry/mass properties of the Apollo Lander [1]

D) Chang'e program

The Chinese Lunar Exploration program (CLEP) also known as Chang'e (Chinese Moon goddess) is a series of missions with the moon objective. The program is divided into 5 phases from 2007 to 2027. The phases are[3]:

Phase 1: Orbital missions.

Phase 2: Soft landers/rovers.

a) Chang'e 3: (*Fig.4*) launched on December 2013, its objective was performing the China's first soft landing on the Moon. Furthermore, carrying a rover and preform exploration tasks. The launching mass was 3800 Kg and the landing mass was 1200 Kg. The main engine can provide from 1500 to 7500 N of thrust. Besides the main engine, it has 28 small attitude thrusters (150 and 10 N) installed on the smaller side panels of the vehicle.

b) Chang'e 4: Initially programmed for 2015, but launched in December 2018 and successfully landed on the far side of the Moon in January. Its geometry was similar (With some adjustments to the mission) to the Chang'e 3 and the propulsion system also. This lander a also carried a rover, Yutu-2.

Phase 3: Sample-return.

Chang'e 5 and 6: It is currently under development and it is intended to be launched by the end of 2019. They will dig and collect about 2 Kg of lunar samples. The mass, geometry and propulsion are planned to be the same as its previous landers, except for the sample return stage.

Phase 4: Lunar research station.

Chang'e 7,8 and 9: They are planned to be launched in 2023, 2024 and 2027 respectively. After this phase they are considering doing a manned mission but still nothing is official.

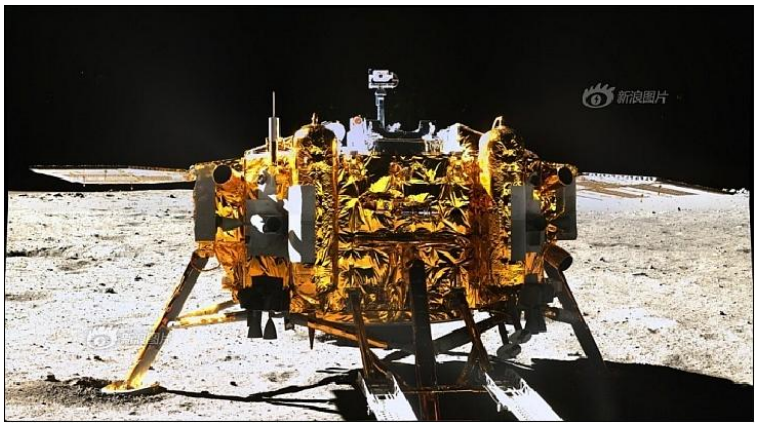

Figure 4: Picture of the Chang'e-3 lander taken by the rover Yutu on the moon on Dec. 15, 2013 (image credit: BACC, CAS)

E) ESA's Lunar Lander (Cancelled)

This is a program started by the European Space Agency (ESA). The objective of the Lunar Lander mission was to show the ability to deliver a payload safely and accurately to the Moon's surface. The mission would have demonstrated the technologies required to achieve a precise soft landing. These technologies will be an asset for future human and robotic exploration missions. However, the project was put on hold at the 2012 ESA Ministerial Council [4].There is also a plan about future missions of mining on the moon.

The main characteristics and geometry is shown on the *Fig.5*. It has 4 legs, five main thrusters and more small attitude control engines. The figure shows a typical configuration of a cluster of thrusters for a lander. The thrusters planned were the EAM (European Apogee Motor) and the ATV (Automated Transfer Vehicle). The landing mass was about 800 Kg and the dimensions were 3.44 of height and 5.6 m of diameter (With legs).

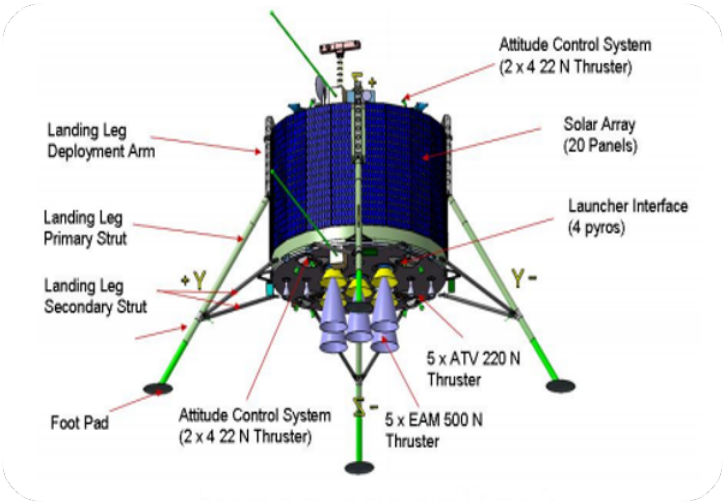

Figure 5: ESA's Lunar Lander characteristics

F) Lunar X-prize

The Lunar X-prize was was a 2007 to 2018 prize space competition organized by the X Prize Foundation, and sponsored by Google. The objectives were to land a robotic spacecraft on the moon, travel 500 meters and transmitting high definition images and video. The economical prize was cancelled but, a few of them still plan to launch their spacecrafts. Some of the main competitors, and the ones which remained more were: SpaceIL, Moon Express, Synergy Moon, Team Indus, Astrobotic and Team Hakuto . Looking at the pictures provided in their websites (*Fig.6*), we can do reverse engineering and have a brief idea of the geometry and configurations.

a) **SpaceIL:** It is a creation of the Israel Space Agency (ISA). As we can see below , it is a small lander with 4 legs, a main engine in the centre and at least 8 small attitude thrusters.

b) **Moon Express:** From Moon express we can see that it is a small lander with four legs and propulsed by a gimbaled big thruster with small attitude thrusters. The goal of this lander was just to land and there were three more projected for the future.

c) **Synergy Moon:** This was a team from USA. We can observe three legged lander, but the propulsion system is impossible to figure out.

d) **Team Indus:** Team Indus is from India and the configuration is a four-legged lander with a gimbaled main thruster

e) **Astrobotic:** This is an USA company which actually plans to send their lunar lander in 2020. The configuration is 5 main pulse-controlled ISE-100 thrusters (660 N each) and 4 attitude thrusters with four legs.

f) **Team Hakuto/Ispace:** It's a Japanese Team managed by Ispace which has good relationship with Astrobotic and they have planned to send its rover into the Astrobotic's Lander. They plan to send their own lander on their next mission, that is why this picture is different, and as we can notice it has four legs. It has a medium size central engine and 5 attitude control thrusters.

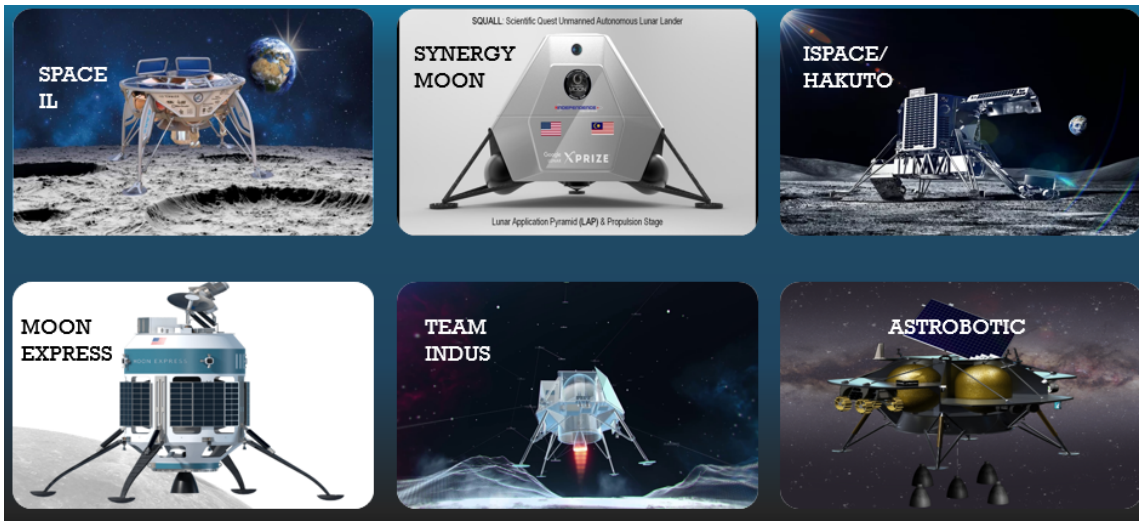

Figure 6: Picture of the X-Prize Landers from their press releases

2.2.2 Rocket Engines for Landers

For this section we consider some of the most relevant rocket engines, and its characteristics for Lunar Landers. Due to the wide variety of mass of the landers the range we've chosen for the main propulsion system is from 2 to 70 kN. Note that some of the exposed are less than this thrust but they are intended to form a cluster of 3 or more of them. The data and pictures shown come from [6].

The first three engines (A,B and C) are pressure-fed designs, using a storable hypergolic bi-propellant. Pressure feeding advantages are the relatively simple system, which makes them low-cost and reliable. The main disadvantage is that the inlet feed pressures are low to limit tank pressure and ensure the tank life. This makes it a bigger engine. Recently, pump-fed (D) engines have been developed, its main characteristics are high specific impulse and more compact engines. However, some other bad characteristics are cost increase and reduced reliability, due to a more complex engine and start-up.

The others (E,F,G) are engines pulse controlled, with several thousands of pulses needed over the life of the spacecraft and small total impulses per activation. These are called Reaction Control Systems. They are pressure-fed, which leads to a relatively large and heavy engine. They commonly use fixed thrust for simplicity reasons. To control the attitude of a lander, a cluster or a network of them have to be part of the propulsion system. At first glance, this option leads to heavier propulsion system.

A) Apollo Descent Propulsion System (DPS)

It was a variable-throttle hypergolic rocket engine manufactured by Space Technology Labora-

tories. It used Aerozine 50 fuel and dinitrogen tetroxide (N_2O_4). It was the predecessor of the TR-201, used for the upper stage of the Delta rocket. This is the highest thrust engine used for lunar landers, as it was a manned mission.

The propulsion system for the descent stage of the lunar module was designed to transfer, from a 110 km circular parking orbit to an elliptical descent orbit with its perilune of 15,000 m, then perform a controlled descent to the lunar surface. To accomplish these maneuvers, they designed a gimbaled pressure-fed ablative cooled engine that was capable of being throttled. A lightweight cryogenic helium pressurization system was also used. The exhaust nozzle extension was designed to break without damaging the LM if it touched the surface, which happened on Apollo 15. The previous Table 1 shows the main propulsion characteristics of this engine.

B) RD-843 (AVUM)

It is currently used as the main engine of Vega's AVUM upper stage. It is a single nozzle liquid propellant rocket engine. It burns pressure-fed Unsymmetrical DiMethyl Hydrazine and nitrogen tetra oxide. It is rated for up to 5 restarts, and can gimbal up to 10 degrees in each direction. A modification of this engine could be used for future manned missions to the moon. The RD843 ground test campaign included 74 tests, 140 ignitions, reaching a total of 8201 s, which is approximately 12 service lives on 4 engines. This data shows the good reliability of this engine.

C) Orbiting Maneuvering System engine (OMS)

It is the engine that provide the thrust needed to perform orbit insertion, transfer, rendezvous and de-orbit of the USA Space Shuttle Orbiter. Each orbiter is equipped with two OMS engines, which are located at the end of the Orbiter. First flight took place in 1981. Each engine could be reused for 100 missions and was capable of a total of 1,000 starts and 15 hours of burn time. The OMS engine is a modification of the Aerojet's Apollo Service propulsion system.

The OMS uses uses an hypergolic bipropellant mix of Nitrogen Tetra Oxide and Mono-Methyl-Hydrazine. The engine assembly is gimbaled by pitch and yaw electromechanical actuators. The gimbal actuation system provides multi-axis gimballing of +-8º.

D) Common Extensible Cryogenic Engine (CECE RL10) [5]

NASA contracted Aerojet Rocketdyne to develop the Common Extensible Cryogenic Engine (CECE), a deep-throttling 15,000 pound thrust class demonstrator rocket engine. A mixture of liquid oxygen and liquid hydrogen.This engine design objective was to perform a wide variety of missions, including human-lunar landings, in-space transfer systems and the exploration of Mars. This engine is an evolution of the RL10, which has earned a reputation of being one of the most reliable, safe and high-performing cryogenic upper stage engines ever developed.

It is a pump-fed, expander cycle engine. This version is throttleable from 30% to 100% and has an extendable nozzle, which increases the usability to lower altitudes specially interesting for single stage landers on planets with dense atmosphere. Without extension, the engine has a nozzle expansion ratio of 4,28 and a length of 1,07m.

E) European Apogee Motor (EAM)

This motor formed part of the European Space Agency's Lunar Lander Propulsion System. The European Apogee Motor (EAM) is a high performance bi-propellant engine operating with the propellants MMH (Monomethyl Hydrazine) and MON (Mixed Oxides of Nitrogen). It's 500N thrust make it suitable in cluster configuration to small landers. It is also called liquid apogee engine (LAE).

The name apogee engine comes from the manoeuvre for which the thruster is typically used, (i.e. a change from an elliptical transition orbit to a circular one). Despite the name, an apogee engine can be used for a range of other manoeuvres, such as Earth orbit escape, end-of-life deorbit, planetary orbit insertion and planetary descent/ascent, which is the case we are interested in.

F) Kaiser-Marquardt R-40B

The model R-40 B bi-propellant engine is designed to perform orbit adjust and perigee thrusts for satellites. A modification of this engine could be used to land small spacecrafts on different planets.

The R-40 is a pressure-fed engine which uses Monomethyl Hydrazine and Nitrogen Tetra Oxide as propellants. The combustion chamber is made of columbium and incorporates radiation and film cooling, which lets the wall reach temperatures up to 1375 K. Adapting the inlet pressure, we can variate approximately 1000 N its thrust. Its length is about 1,3 m and a maximum diameter of 0,66 m.

G) Aerojet Rocketdyne RS-41

This engine developed by Rocketdyne is relatively high thrust for attitude control systems. Its 11000 N thrust could make it suitable with a cluster of engines configuration for the bigger moon landers. It is a bipropellant engine, and like most Rocketdyne's engine works with a mixture of Nitrogen Tetra Oxide and Monomethyl Hydrazine. It has a relatively high weight compared with the other small RCS (68,95 Kg) and its lifespan is approximately 2000 s.

2.3 Thrust vector control

There are four main configurations of Thrust Vector Control (i.e. ability of a rocket, or other vehicle to manipulate the direction of the thrust from its engines in order to control the attitude or angular velocity of the vehicle). The following figure (*Fig.7*) shows the basic configurations and principles of thrust vectoring.

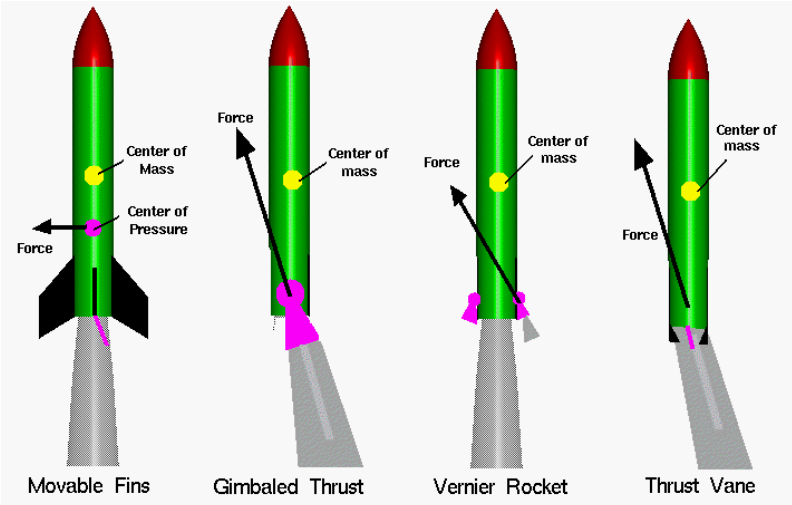

Figure 7: Four typical configurations of TVC in rockets. Source: NASA

2.3.1 Gimbaled thruster

The engine, is controlled by electro mechanical or hydraulic actuators, in order to orientate the nozzle to control the attitude of landers. Considering that the rotation center coincides with the center of gravity (C.o.G.), since thrust no longer passes through the center of mass, a torque is generated and the nose of the rocket (in our case lander) turns to the right (*Fig.7*).

For lower stages this is the most common attitude control system, because they are solid engines, thus there is no possibility of a fast turn on/off. This configuration was used for the Apollo Lander. It isn't very common in lunar landers because most of the existent landers have low payload mass. This explains why this configuration has only been used for Apollo lander, because it was a manned mission with high mass/thrust requirements. For future manned missions, or high payloads necessary to colonize other planetary bodies, it's an attractive design solution.

2.3.2 Thruster Cluster

The principle is to distribute a set of small thrusters, so that if one of them is on (e.g right thruster) and the other is off (e.g left), the force is no longer passing through the center of mass and the situation is similar to the gimbaled configuration. Rockets are usually pulse-controlled.

For small landers it is the most common configuration, as there is no need of high thrust. However, the bigger is the payload mass, more thrust is required, thus more/bigger engines are needed, and the relationship between the dry mass and the total mass of the whole spacecraft increases. Thus, there is less available mass for fuel or payload.

2.3.3 Comparison of both configurations

The main advantages of gimbaled thruster compared with the cluster thruster:

- Only one Thruster: This reduces the total dry mass as bigger engines usually have better thrust to weight ratio, it also results in lower costs.
- Variable throttle: The engine used has the ability to adapt to different thrust requirements, this can save fuel.

The main disadvantages of gimbaled thruster compared with the cluster thruster:

- Response time: Given that it has to rotate into position to apply thrust, makes it less responsive.
- Redundancy: The actuators and the main engine are critical, and a failure in one of this systems results in an uncontrollable lander. With a cluster you can use redundant engines to increase safety.

3 Description of the landing characteristics

In this chapter we describe the different aspects which will define the model and the different parameters taken into account. As it is a well known practical case, I've used most of the Apollo data shared by NASA [1].

3.1 Trajectory and phases of the landing

This project starts at the terminal phase of the Apollo Lunar Module. However, there are three phases braking, approach and terminal phase. The image below shows a summary of the phases of landing [7]. Note that all the data used in the following tables is used in the model to classify the different phases.

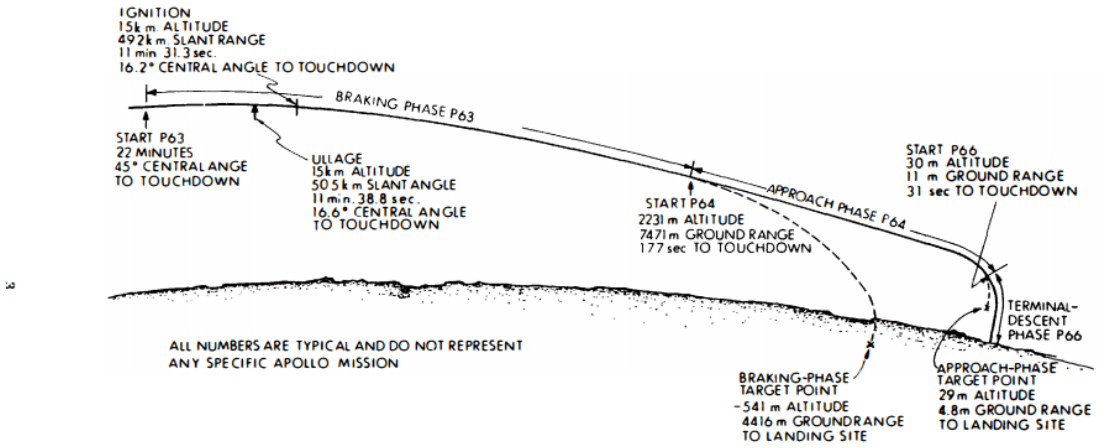

Figure 8: Typical trajectory of the Apollo landing stage. Source: NASA

3.1.1 Phase 1: Braking

This phase starts at the height of 50.000 ft (15000 m approx.), the lander is oriented at 180° and in this phase the objective is to reduce the lateral speed, (i.e. Vx). There are also side objectives, such as reduce the fuel consumption, and keep the attitude of the lander controlled.

Phase 1: Braking		
Starting Altitude [m]	15000	
End of the phase [m]	7010	
Vertical velocity (Vz) $[m/s]$	$Vz_{p1,0} = 0$	$Vz_{p1,f} \approx -126$
Horizontal Velocity (Vx) $[m/s]$	$Vx_{p1,0} = 1671.5$	$Vx_{p1,f} < 160$
Roll angle (Φ)[°] (*For all phases*)	$\Phi_0 = 0$	$\Phi_f = 0$
Pitch angle (Θ)[°]	$\Theta_{p1,0} = 90$	$\Theta_{p1,f} = 60$

Table 2: Summarizing table of the different trajectory parameters of the braking phase. **Definition of the reference axes in the Section 4.3.1.*

3.1.2 Phase 2: Approach

In this phase the most important parameter is the orientation of the lander. It has to lose most of its lateral speed and orientate vertically to start the terminal phase in order to land. As secondary objectives we have the vertical, lateral velocity and fuel consumption.

Phase 2: Approach		
Starting Altitude [m]	7010	
End of the phase [m]	200	
Vertical velocity (Vz) $[m/s]$	$Vz_{p2,0} \approx -126$	$Vz_{p2,f} \approx -6.7$
Horizontal Velocity (Vx) $[m/s]$	$Vx_{p2,0} < 160$	$Vx_{p2,f} < 20$
Pitch angle (Θ)[º]	$\Theta_{p2,0} = 60$	$\Theta_{p2,f} = 20$

Table 3: Summarizing table of the different trajectory parameters of the approach phase.

3.1.3 Phase 3: Terminal

Finally, at approx. 200m the lander is vertically oriented and it is ready to decelerate to soft land on the Moon. The most important/critical parameters is the vertical velocity and the vertical orientation. This is one of the most critical phases because if the lander touches the surface at high speeds, the result could be damage on the structure, thus the failure of all the mission. When the lander is close to the surface (1.5 m) the engines shut down and there is a free fall that the structure has to bear.

Phase 3: Terminal		
Starting Altitude [m]	200	
End of the phase [m]	1.5	
Vertical velocity (Vz) $[m/s]$	$Vz_{p3,0} \approx -6.7$	$Vz_{p3,f} < 2$
Horizontal Velocity (Vx) $[m/s]$	$Vx_{p3,0} < 20$	$Vx_{p3,f} < 1$
Pitch angle (Θ)[º]	$\Theta_{p3,0} = 20$	$\Theta_{p3,f} = 0$

Table 4: Summarizing table of the different trajectory parameters of the terminal phase.

3.1.4 Successful landing criteria

Taken from [8], we can see the figure 9 which is the doghouse plot of the landing. This is the acceptable and optimal vertical an horizontal speeds which wouldn't cause any damage on the structure, thus the soft landing could be considered a success. The ellipse represents the relations of speeds that would make a 99,74 % of probabilities of a good landing. Apart from this, the max angle related to the vertical can't be greater than 10^{o}.

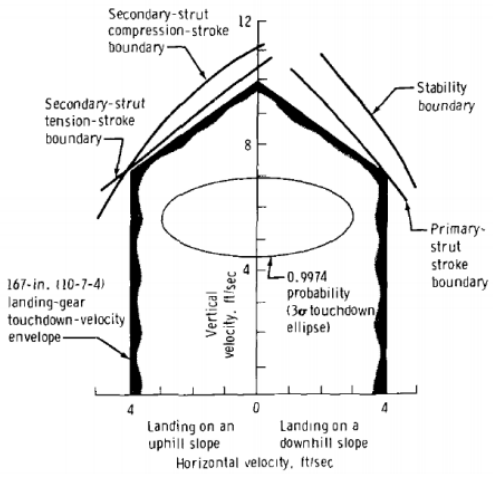

Figure 9: Doghouse plot of the Lunar Descen Module [8]. Note that the units are feet/second.

3.2 Parameters

To be able to compare both design options quantitatively we have to set the relevant parameters we are going to change in order to optimize the dynamic performance. Amongst all the different design parameters that must be taken into account we've chosen the most relevant ones so that it can be applied to the majority of the landers:

- The total mass
- The maximum thrust

The geometry and other aspects of the mission remain the same, to see how these two affect the attitude of the lander.

3.2.1 Total mass

Instead of changing the mass of each component proportionally, the only part that changes its mass (without changing its center of gravity) is the body frame, which involves all the subsystems and the payload carried. Accordingly, the inertia would also be changed. Then, inertia coefficients are proportional to the mass, thus the inertia matrix in this model is also proportional to the total mass of the lander.

However, in reality the different mass requirements would have the result of different design choices, such as different geometry, different mass distribution, different engines... (i.e. it's not the same size of lander for a rover mission or for a manned mission).

The lander which performed the lightest soft moon landing is the Surveyor with 292 Kg. So, we can set the iteration of mass start at 500 Kg. The heaviest lander to succeed was the Apollo

program which had around 17,000 Kg in total (Ascent and descent modules). However, like the biggest engine considered (CECE RL10) is about 67,000 N we can set with a decent margin the maximum mass at 25,000 Kg.
**Note that all the masses are with the tanks full.*

3.2.2 Maximum thrust

Like the mass variety is broad (500-25000 Kg), we have used three engines to variate the maximum thrust, so that a 500 kg lander doesn't have a 40kN engine because that would be disproportional. First, we make a comparison of the different available motors that could fit in our lander, and also is a way to compare the different possible configurations.

For the smaller landers we are considering usual engines, but for larger landers, historically, the only high thrust one used is the Apollo's descent engine. Thus, we'll use upper stages engines of Vega or other launchers, which could be modified for landing missions.

Engines	**Vac. Thrust[N]**	**Spec. Impulse [s]**	**Thrust to weight ratio[-]**	**Thrust Vector Control**
CECE	66,700	412	51.9	-
Aestus II	46,000	337.5	31.7	+-6° pitch and yaw
R-40B	4000	303	30	-
DPS	44,037	311	25.65	+-6° pitch and yaw
OMS	26,700	316	23.3	+-6° pitch and +-7° yaw
R-42	890	303	20	-
RS-41	11,100	312	16.43	-
RS-21	1,330	294	16.18	-
RD-843(AVUM)	2,452	315.5	15.71	+-10° pitch and yaw
EAM	425	321	10.44	-

Table 5: Comparison of different rocket engines for Lunar Landers. Adaptation from [6]

4 Model and Control of the Lander

Modeling phase is the analytical, numerical or symbolical process which, once and for all, sets up the equations of motion describing a multibody system for a given set of system parameters and generalized coordinates.

4.1 Multibody Dynamics

To simulate the model, we have used a symbolic multibody dynamics software called ROBOTRAN [9]. For instance, the direct dynamic model (The one used for the project) can be seen as a black box whose input are the system parameters (joints location, body masses, and inertia, etc.) and the generalized positions q and velocities $\dot{q}$ and whose outputs are the generalized accelerations $\ddot{q}$ and the Lagrange multipliers λ.

Symbolic generation of multibody models tries to take advantage of numerical techniques. So called symbolic multibody programs manipulate only arithmetical operators and strings of alphanumeric characters to generate the analytical form of the equations using a desired syntax (e.g. C, Java, Fortran, MATLAB, etc.). For a given multibody application, this symbolic generation is performed only once, as in manual generation, this characteristic saves a lot of computation time. From the multibody modelling point of view, these symbolic generators exhibit the same level of generality as their numerical competitors in the sense that they can handle systems with any topology and containing several degrees of freedom. However, they allow drastic simplifications, from the most trivial (addition/multiplication by zero) to the most complex ones (simplification of long trigonometric expressions).

If we analyze and compare multibody symbolic software, the common attribute is their intrinsic versatility in terms of:

- Model type and underlying formalisms (inverse or direct models, kinematic, dynamic equations, sensitivity matrices, etc.).
- Wide diversity of languages

ROBOTRAN is based on the use of relative joint coordinates. As usual in this case, equations are, if needed established for a tree-like structure (i.e. with no explicit constraints).

4.2 Assumptions and Hypothesis

1. The assumptions related to the moon are:
    - Plane surface without craters or other geographic features.
    - Constant gravity: -1,62 $\frac{m}{s^2}$
    - No lunar soil
    - No atmosphere
    - Moon's surface properties known (Taken from apollo experimental data of the footprints) (*Table 6*).

2. The assumptions on the Lander are:

    - Solid rigid body
    - No Joint Friction
    - Same geometry for all tests, independent on the mass: the only changes are related to the different configurations.
    - The motors are a resultant of forces (no thermodynamics approach).
    - The landing body structure is simplified (Just four straight legs).
    - The frame rigidity is simplified as two springs (one for each degree of freedom) on the Legs-Body union.

3. The Fuel consumption assumptions are:

    - The change of mass doesn't affect the position of the center of gravity: this assumption can be done because as first results showed, the computed phase consumes less than 3% of total fuel tanks, thus the variation of CoG can be neglected.
    - The fuel/oxidizer consumption is linear with thrust and proportional to the time of the burns. The size of the tanks is proportional to the total mass of the lander (keeps the same relation with it).
    - Both configurations use the same tanks of the Apollo and same propellant/oxidizer.
    - There is no start/stop delay to operate the engine.

4. About the actuators:

    - They don't have delay on the change of position. (Usually it is <1s).
    - The initial configuration is at the neutral point.
    - The energy needed to control them is not computed.
    - One of the two parts includes the mass of the integrated power and drive unit of SABCA.

5. About the "Manned missions"

    - To asses the acceptability of a mission, there is a sensor which measures the accelerations humans would suffer.

Moon's surface properties	
Dynamic friction coefficient	0.4
Static friction coefficient	0.85
Stiffness coefficient	41250 N/m
Damping coeff. (1% of stiffness coef.)	412.5 Ns/m

Table 6: Moon's surface properties computed from the mean size of 776 footprints.

* We consider the resultant force of the ground as a linear spring-damper given by the stiffness and damping coefficient. The procedure to compute it is to measure the mean value of the depth of the footprint ($\Delta\bar{X}$). After that we know that the mass of the astronaut with the space suit is 200 Kg. With this values we calculate the mean stiffness and estimate the damping coefficient as a 1% of the stiffness constant.

4.3 Model of two configurations

4.3.1 Reference axis and common geometry for both models

The first step to define the geometry of the lander is setting the reference frame of the main body, these are defined as the following diagram of the lander.

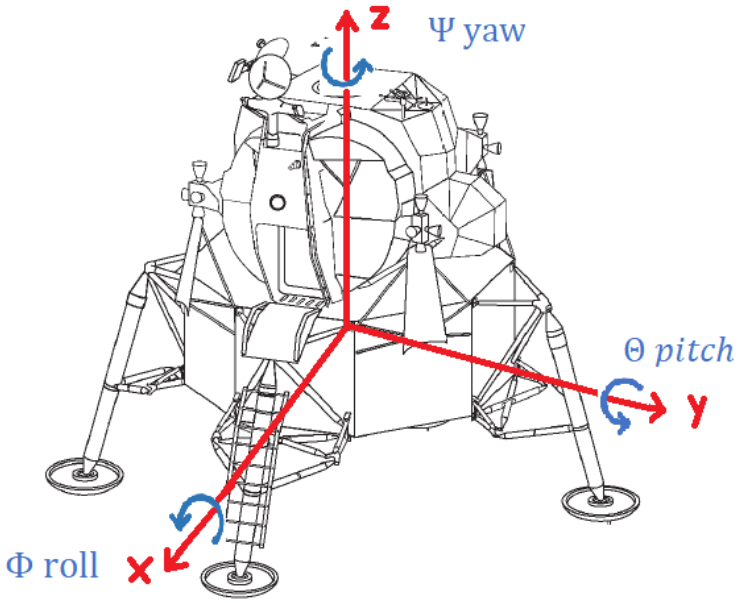

Figure 10: Geometry and reference axis of the main body. Adaptation from [1]

The main body as well as the legs are common for both configurations, so we'll define all the relevant points (relative coordinates) and a summary scheme of the whole lander.

Point	Coordinates (x,y,z) [m]	Reference
Main Body		
C.o.G. of the frame (1)	(0,0,1.4)	Body Axes
Human sensor (2)	(0,0,2)	Body Axes
Leg union points* (7,9,11,13)	(±4.7244,±4.7244,0)	Body Axes
Legs		
Leg's C.o.G. (3,4,5,6)	(0,0,-2)	Leg union points
Ground Contact points(8,19,12,14)	(0,0,-4)	Leg union points

Table 7: Relative coordinates of the points defining the model. ** Note that the points are the four possible combinations of the coordinates signs*

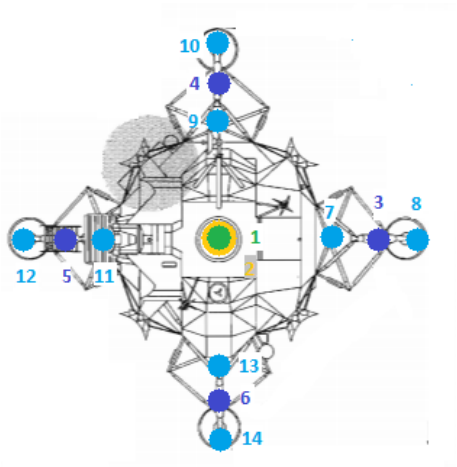

Figure 11: Diagram of relevant Points on the lander. In green the C.o.G. of the frame, in yellow the sensor, in light blue the leg points and in dark blue the C.o.G. of the Legs. Adaptation from [1]

4.3.2 Thruster Cluster

This layout has the 6 Degrees of freedom for the main structure (From now on D.o.f.), these are Tx ,Ty, Tz, Rx, Ry, Rz (T for translation in the respective axis and R for rotation in the respective axis). It has five fixed thrusters (i.e. no movement of the engines) to the frame which are pulse-controlled . Finally, the 4 legs, each one is attached with a ball joint to the main body.

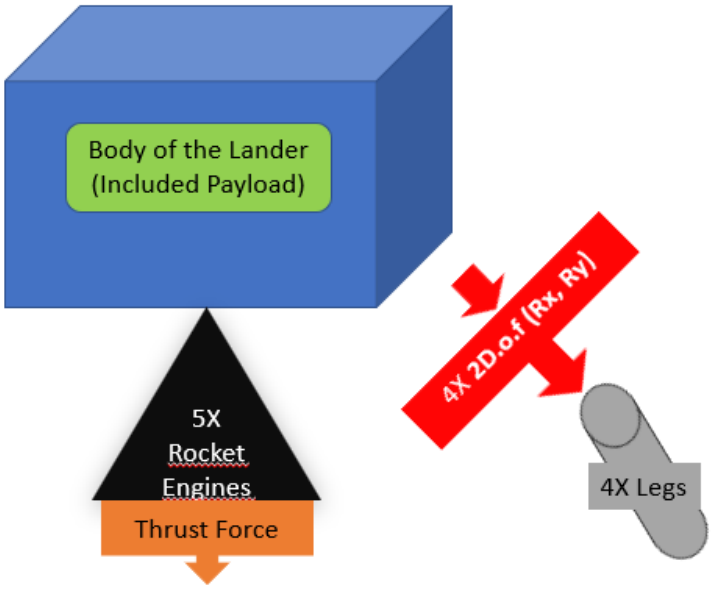

Figure 12: Diagram of the Thruster Cluster configuration.

Regarding the points defined, there are only 5 more points related to the existence of the thrusters, thus there is an external force on each of them.

Point	Coordinates (x,y,z) [m]	Reference
Main Body		
Center Thruster (14)	(0,0,0)	Body Frame
Lateral Thrusters (15,16,17,18)	($\pm$2,$\pm$2,0)	Body Frame

Table 8: Relative coordinates of the points defining the position of the thrusters. ** Note that the points are the four possible combinations of the coordinates signs*

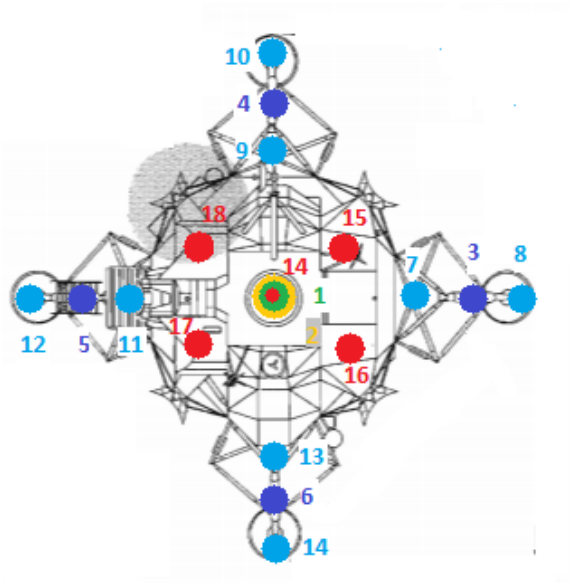

Figure 13: Diagram of the Thruster positions, in red the Thrusters. Adaptation from [1]

Finally, the choice of engines for this configuration summarized in the table below, which have been chosen as a result of computing the total thrust needed to lift the whole lander, plus a minimum extra 40% of thrust capability to ensure the controllability.

Thruster	Range of lander masses [Kg]	Maximum Thrust [N]
RS-41	$25,000 > M > 10,000$	11,100
RB 40B	$10,000 > M > 4,000$	4,000
AVUM RD-843	$4,000 > M > 900$	2,452
EAM	$900 > M$	425

Table 9: Thruster Cluster chosen engines to compute simulations.

4.3.3 Gimbaled thruster

This layout has the 6 d.o.f for the main structure , these are Tx,Ty, Tz, Rx, Ry, Rz . It has two actuators and they have 5 d.o.f. (two ball joints without Rz at each end as the figure shows). The engine is attached also with a ball joint with the Rz blocked, so that is 2 d.o.f more. Finally, the 4 legs, each one is attached with a ball joint to the main body.

The actuator is divided into two parts which move relatively and are controlled electrically. In our model we control the position of Tz, so that we can operate the 2 d.o.f (one with each actuator) of the engine-body union, thus control the whole attitude of the spacecraft.

Due to the interest of SABCA in this project we chose the values of its low power TVC which has a length 251 mm and a stroke of 75 mm.

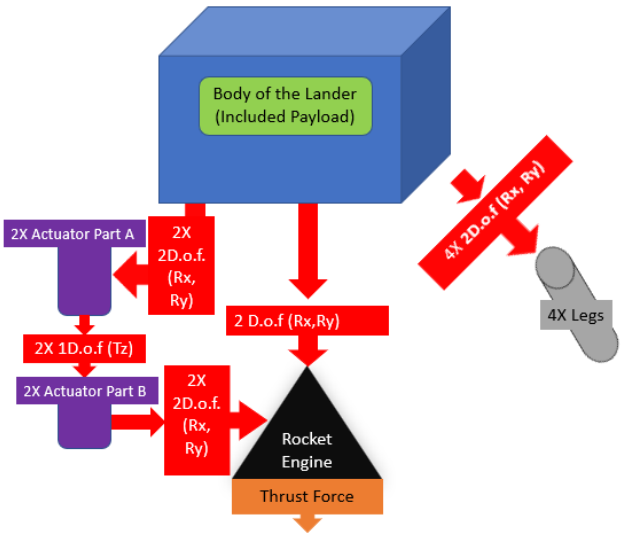

Figure 14: Diagram of the Gimbaled Thruster configuration.

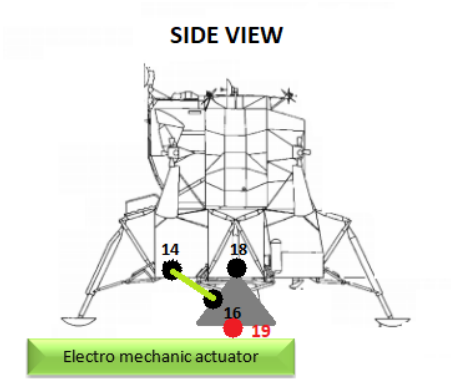

Figure 15: Side view of the Thruster and actuators. Adaptation from [1]

Regarding the points defined generically, there are 6 more points related to the position of the actuators and thruster. Notice that the points 14 and 16 are the attachment points A and B of the X axis actuator (Similar with 15(A), 17(B) with Y axis actuator). Note that the middle actuator point is same for part A and B in neutral position, but when the actuators extends or contracts, the Tz defines the distance between A and B parts.

Point	Coordinates (x,y,z) [m]	Reference
Main Body		
Actuator attachment point(A) (14,15)	(-0.355,0,0);(0,-0.355,0)	Body Frame
Thruster attachment point (18)	(0,0,0)	Body Frame
Thruster		
Thruster attachment point (B) (16,17)	(-0.185,0,-0.185);(0,-0.185,-0.185)	Thruster attachment point
Force point (19)	(0,0,-2.413)	Thruster attachment point
Actuator		
Middle actuator point (20,21)	(0,0,-0.1255)	Actuator attachment point(A) (14,15)

Table 10: Relative coordinates of the points defining the Gimbaled Thruster Configuration.*Middle points of the actuators not shown in the figure for clarity.

Again, the election of engines for this configuration summarized in the table below.

Thruster	Range of lander masses [Kg]	Maximum Thrust [kN]
CECE RL-10	$25,000 > M > 10,000$	66,700
OMS	$10,000 > M > 4,000$	26,700
RS-41	$4,000 > M > 900$	11100
AVUM RD-843	$900 > M$	2,452

Table 11: Gimbaled Cluster chosen engines to compute simulations.

4.4 Mass properties

For this section, we summarize the main mass properties on the tables below. We have to take into account that positions are relative. Note that repeated bodies (e.g. Legs, actuators ...) have same mass properties.

Body	**Total mass [Kg]**	**Position CoG (x, y, z) [m]**	**Inertia** $(I_x, I_y, I_z, I_{xy}, I_{xz}, I_{yz})$**[Kg** m^2]
Common for both models			
Main Frame	16437 *	(0, 0, 1.4)	(35060, 37101, 35410, 118, 698, 260)*
Legs	55	(0, 0, -2)	(992, 457, 442, 0, 0, 0)
Gimbaled Thruster			
Engine	**	(0, 0, -1.81)	(450, 450, 100, 0, 0, 0)
Actuators A	9.6	(0, 0, 0)	(0.0975 , 0.0975 , 0.0975 , 0, 0, 0)
Actuators B	3.7	(0, 0, 0)	(0.0975 , 0.0975 , 0.0975 , 0, 0, 0)

Table 12: Mass and inertia properties of the model. *(*) This parameters change proportionally with the mass, these are reference values from the apollo.(**) The engine's weight is changed for each model of engine (see Table 5)*

4.5 External and internal forces

1. **External Forces**
   - Constant gravity: -1,62 $\frac{m}{s^2}$
   - Engines' thrust
   - Ground Normal Force: If the lander is touching the floor, there is a force applied on the contact points.
2. **Internal Forces**
   - Torsion spring-damper on the leg-frame union: simulates the landing frame rigidity. The constants used for this are K=100$\frac{kN}{m}$, C=10$\frac{kNs}{m}$, Natural length=0.5236 rad
   - Actuators: Although we control the position of the actuators, this constraint generates an internal force that the actuator has to resist.

4.6 Control

The aim of this thesis is to set a detailed first model but time limitations lead us to a relatively basic control. Thus, the control isn't the optimal one for this problem. The way we control both configurations is part of the linear control theory , which supposes that the variations of the variables are close to the objective one, and the outputs are proportional to the inputs.

4.6.1 Gimbaled thruster

Due to the complexity of the interaction between the length of the actuator and thrust (i.e. if the thruster is off, the length of the actuator doesn't change the attitude of the lander), we developed one of the simplest closed loop controls. The Proportional Derivative control (PD).

A PD controller calculates an error value e(t) as the difference between a desired value of a variable and the measured variable and applies a correction based on proportional, and derivative (derivate of the error $\dot{e}$) terms (P and D respectively), hence the name.

This feedback mechanism doesn't guarantee the stability or the optimal solution for the control, but it's a first step to be able to study the dynamics of the Lander. The process to "tune" the constants is iterative, and depends on the control designer.

$$u(t) = K_p e(t) + K_d \frac{de(t)}{dt}$$

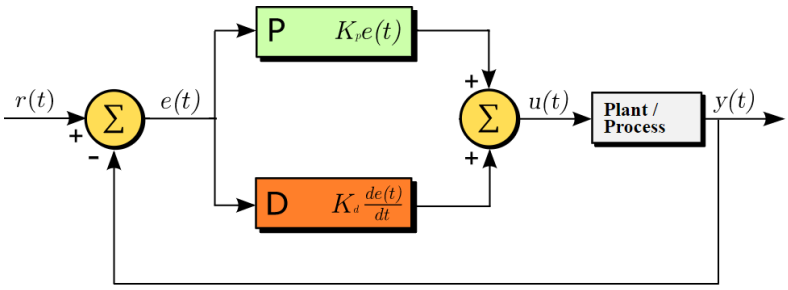

Figure 16: PD controller close loop scheme. Adaptation from Wikipedia

In this case the implemented PD control relations are the error of the descent velocity with the thrust and position error with the actuators, thus.

$$A.length_X = P_\Theta * e(\Theta) + D_\Theta * e(\dot{\Theta})$$

$$Thrust = -(P_{Thrust} * e(\dot{Z}) + D_{Thrust} * e(\ddot{Z})) * Thrust_{MAX}$$

Where the maximum actuator length is 37.5 mm on each side and the maximum thrust($Thrust_{MAX}$) is given by the engine.

4.6.2 Cluster of engines

From the control point of view, this model is more simple than the other. We took the decision to make a little more complex control, the **Linear Quadratic Regulator (LQR)**. This is part of the theory of optimal control, concerned with operating a dynamic system at minimum cost. The LQR algorithm decreases the work done by the engineer to optimize the controller. However, the control designer still needs to specify the cost function parameters, and compare the results with specified design goals. This means that the parameter definition is an iterative process in which

the engineer judges the "optimal" controllers produced through simulation and then adjusts the parameters to produce a controller more consistent with goals.

Linear Quadratic Regulator (LQR)

For a discrete time linear system defined as:

$$x_{k+1} = Ax_k + Bu_k$$

Where x is the state vector and u is the input vector. x_{k+1} is the variation of the state vector and A and B are the linear relations of the variation with the state and inputs respectively.

The cost function computes the 'desired weight' of each of the states (Q) or inputs (R) in the control and is defined as:

$$J = x_N^T Q x_N + \sum_{k=0}^{N-1} (x_k^T Q x_k x_k^T + u_k^T R x_k u_k^T)$$

This means that if, for example we want to minimize the actuator effort (in our case is thrust which can be easily related to fuel consumption), we will increase the values of R. On the other hand if we want to increase the performance (Minimize the error on position or velocity), we will increase the values of Q. If the system is stable J is a bounded summation and $(x_k^T Q x_k x_k^T, u_k^T R x_k u_k^T) > 0$.

And the optimal control sequence minimizing the performance is:

$$u_k = -F_k x_k$$

Where F_k has been computed using 'lqr' function in MATLAB, which calculates the eigenvalues which minimize the cost function and stabilizes the system, given the system matrices(A,B) and the desired Q and R matrices.

A and B Computation

Before using the 'lqr' function we have to define the system we are going to control. To do so we consider the system in defined as its semi-explicit direct dynamics model, as it is defined in ROBOTRAN [9].

$$M(q, \delta) + c(q, \dot{q}, \delta, fr, tr, g) = \Phi(q, \dot{q})$$

– M : is the generalized mass matrix of the system (which is symmetric and positive definite)

– c : is the non linear dynamic vector which contains the gyroscopic, centrifugal effects as well as the contribution of gravity g, external resultant forces f r and torques tr,

– q : denotes the relative generalized coordinates,

– δ : gathers together the dynamic parameters of the system (body masses, centers of mass location and the six components of body tensors inertia

– Φ : represents the generalized joint forces (torques): their explicit computation is typical in relative coordinate formulations, the reason being strongly related to robotic applications and inverse dynamics issues.

To do so, we use the obtain the initial c matrix by using the 'mbs_dirdyna_NAME' function implemented in ROBOTRAN. Then, we aim to express our system as a linearalized one with a Damping Matrix (G), a Stiffness Matrix (K) and the generalized Mass Matrix (Mr):

$$M_r\ddot{q} + G\dot{q} + Kq = 0$$

If we consider as an approximation that for smalls variations of q:

$$\frac{\delta c}{\delta q} \simeq \frac{\Delta c}{\Delta q} = K$$

Same for the damping matrix:

$$\frac{\delta c}{\delta \dot{q}} \simeq \frac{\Delta c}{\Delta \dot{q}} = G$$

With a $\Delta\dot{q} = \Delta q = 10^{-5}$ we obtain, running again 'mbs_dirdyna_NAME' function, the matrices K and G. Then, we can obtain the Matrix A as follows:

$$\begin{bmatrix} 0 & M_r \\ M_r & G \end{bmatrix} \dot{x} + \begin{bmatrix} -M_r & 0 \\ 0 & K \end{bmatrix} x = 0$$

$$\dot{x} = (-\begin{bmatrix} 0 & M_r \\ M_r & G \end{bmatrix}^{-1} \begin{bmatrix} -M_r & 0 \\ 0 & K \end{bmatrix})x = Ax$$

For the B matrix we follow the same procedure but instead of generalized coordinates q we use the linearization of the outputs (u) so that.

$$\dot{x} = Bu$$

In our case, like the mass changes (due to iteration and fuel consumption), we can't use the same matrices for all the masses. Thus, the solution we propose is to create a database of F_k matrices (In MATLAB file called K), so that for each mass there is already an optimal control matrix computed. We have to notice that time in the simulation is discrete, and the number of computed matrices can't be infinite. Thus, we computed 523 matrices in between minimum and maximum mass (500-25,000Kg) to assure that for all the masses, the error on mass on computed matrices would be as low as possible. Using this database also saves computation time (Matrices are precomputed).

5 Results and analysis

In this chapter, after obtaining the data of simulations, we analyse it and extract some conclusions and possible future improvements of this developed model.

5.1 Lander dynamics

The data used for this section is taken from the Apollo Descent Module (Mass). About the global dynamics of the lander (*Fig.18* and *Fig.20*) we have to highlight that the engines shut down before touching the ground at an altitude of 3.5 meters. This causes the increase of vertical velocity before decreasing it dramatically when the lander touches the ground.

5.1.1 Gimbaled Thruster

The characteristics of this model, should make it in practice it's actuations a little bit slower due to the delay of actuators to reach the desired position, a problem that in cluster thruster configuration you don't have.

As we can see at (*Fig.17*) , the initial position of the Lander is at 20º and, in order to reach the landing position (Vertical), the actuators are fully extended, thus the thruster rotation is at it's maximum (Around 9º). Note that there is a little bit of delay between the immediate position of the thruster and the start of rotary motion of the lander. This can be explained by the control used, the PD. As the force of the thruster is controlled by the vertical speed, and the initial vertical speed error is not enough, the force applied is too low (or zero) to change significantly the attitude of the lander. Stable phase is reached after 8 seconds approximately.

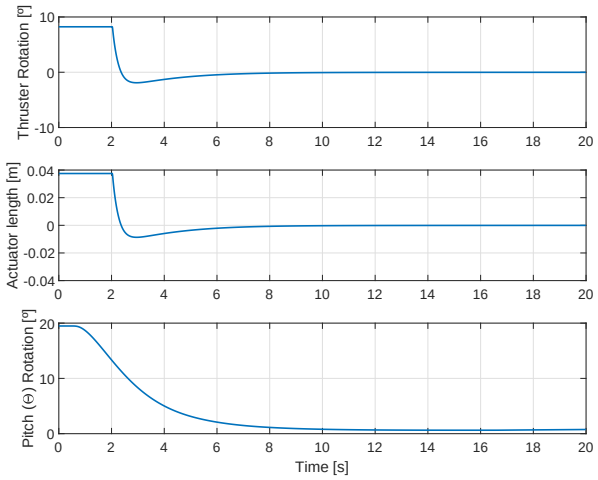

Figure 17: Actuators in a 20º turn, with the mass of Apollo Lander. (a) Thruster rotation, (b) Length of the actuator, (c) Pitch rotation of the Lander

At the Fig.18, we can observe a change of velocity at 30 meters, imposed by the control, to decelerate before reaching the ground. The change can be easily noticed looking at the thruster graph which has a peak when this condition is reached. If this braking is done too early, the lander will take too much time at the final descent,and would increase the fuel consumption. If it's too late, the lander will reach the ground at high speed and this could damage the lander or the payload (critical for manned missions). We can see that the altitude chosen isn't optimal because the lander could brake later, but this is because for bigger masses the engine is the same, and the transition phase takes more time with the same values. The main goal was to successfully land all the computed landers, not the optimal solution. Hence, in future versions of this model, it'd be a good idea to optimize the trajectory to reduce the fuel consumption and optimized for each mass.

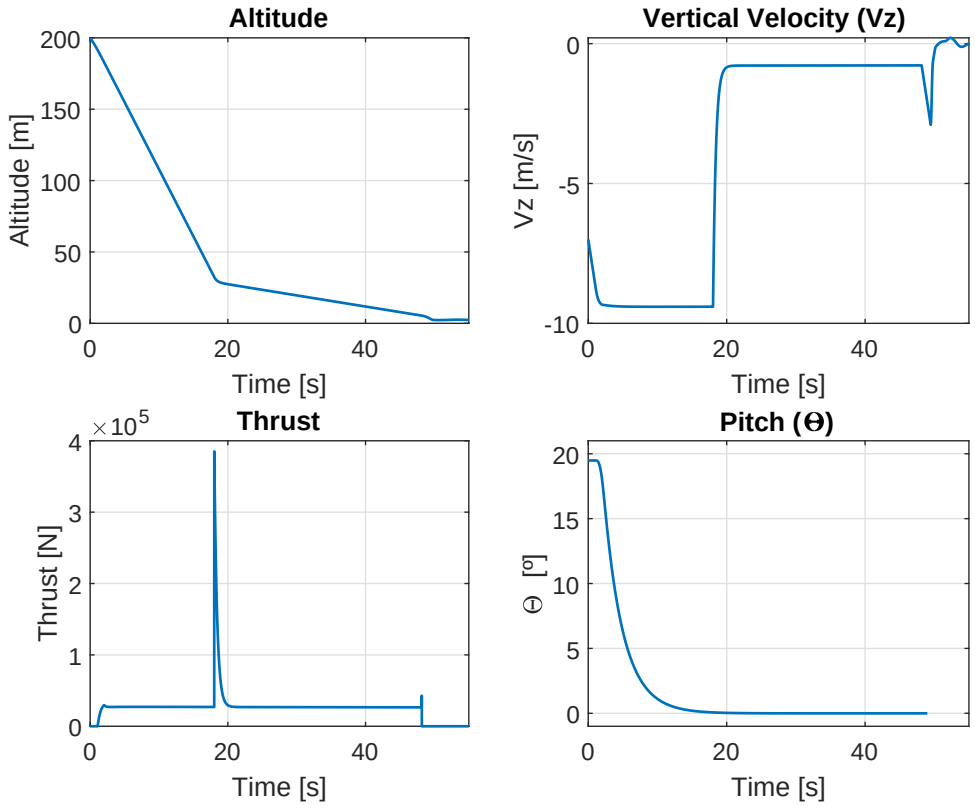

Figure 18: Dynamics of Gimbaled Thruster, with the mass of Apollo Lander. (Top left) Altitude of the lander. (Top right) Vertical Velocity.(Bottom left) Thrust. (Bottom right) Pitch angle

5.1.2 Cluster Thruster

On the other hand, the cluster thruster configuration uses the difference on the forces applied by each of the thrusters to perform the actuations.

At the Fig.19, we observe that Thruster 2 and Thruster 4 are antagonists, as expected. This means that, if there is a difference on thrust of these engines, (Thruster 2 > Thruster 4) there is a negative variation on the pitch motion ($\frac{d\Theta}{dt} < 0$). If both have the same Thrust, they only contribute to the vertical velocity. Same happens with Thruster 1 and 3 on Roll motion. The central thruster just contributes to vertical motion. Indeed, the activation of the Central engine doesn't create any torque as the force is aligned with the C.o.G of the lander.

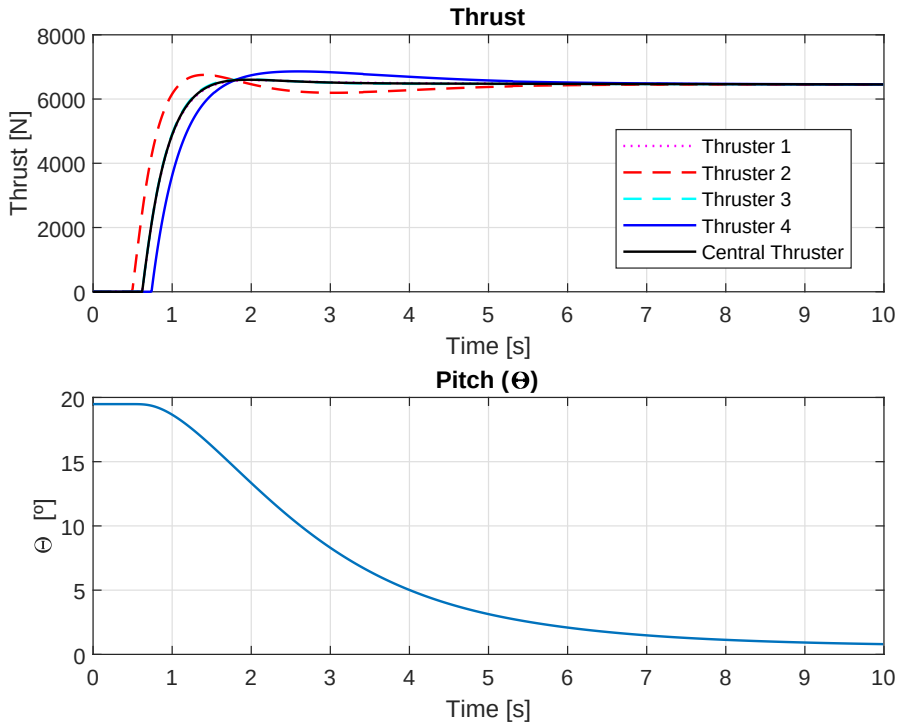

Figure 19: Lander in a 20º turn, with the mass of Apollo Lander.. (a) Thrusters force, (b) Pitch rotation of the Lander .* *Note hat the total Thrust is the sum of the 5 Thrusters*

On Fig.20, we can also see the change of velocity at 35 meters but, in this case it is a more gradual change due to the optimization of fuel consumption made by LQR. There is a small Pitch variation when the lander touches the ground which is related to the stiffness of the torsional springs modelled in the legs. This part is out of the scope of this thesis because the goal was to land with the safety criteria parameters and the behaviour once it touches the ground isn't representative as this isn't a structural model. With same initial conditions we see a faster landing

(almost 10 seconds of difference). This is because the transition in Vertical velocity is more gradual which saves fuel and reduces the accelerations suffered.

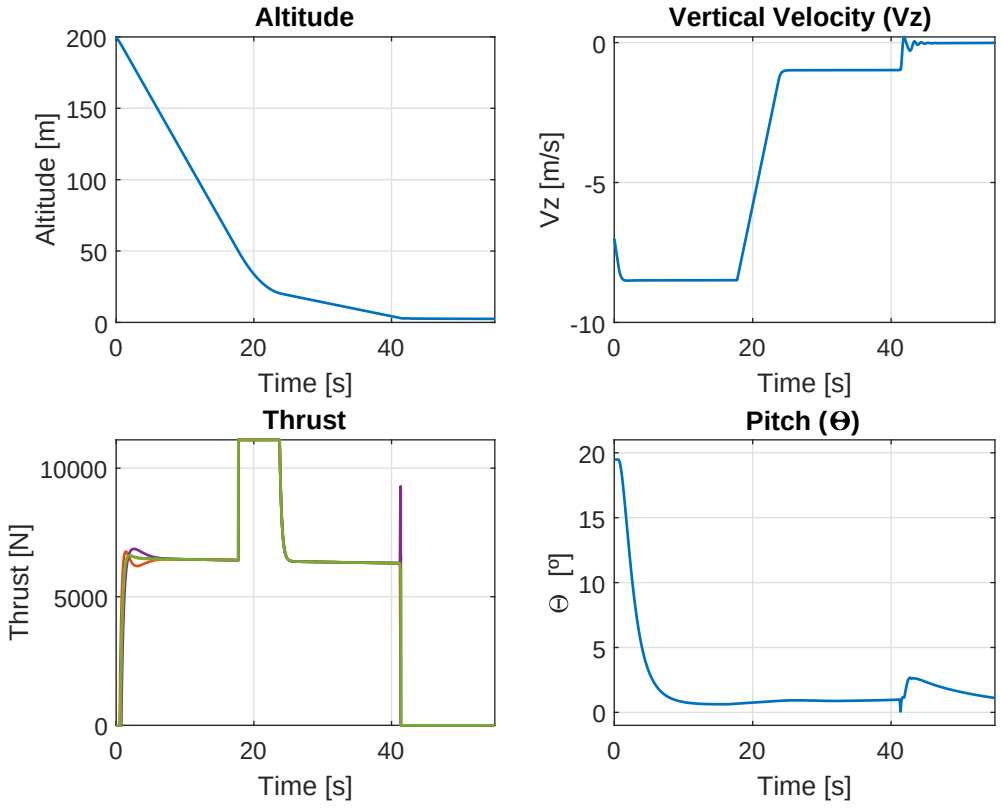

Figure 20: Dynamics of Cluster Thruster. (Top left) Altitude of the lander. (Top right) Vertical Velocity.(Bottom left) Thrust. (Bottom right) Pitch angle.* *Note hat the total Thrust is the sum of the 5 Thrusters*

5.1.3 Dynamics Comparison

Due to the different characteristics of both controllers, we can't take this comparison as very accurate, indeed the dynamics depend on designer's choice. Anyway, we can highlight some differences between both configurations.

Comparing rotation dynamics on Fig.20 we can conclude that:

-Cluster thruster configuration reaches before the steady state. However, the error with desired equilibrium value ($\Theta = 0$) is bigger.

-Both configurations have an acceptable error on position always less than 1^o.

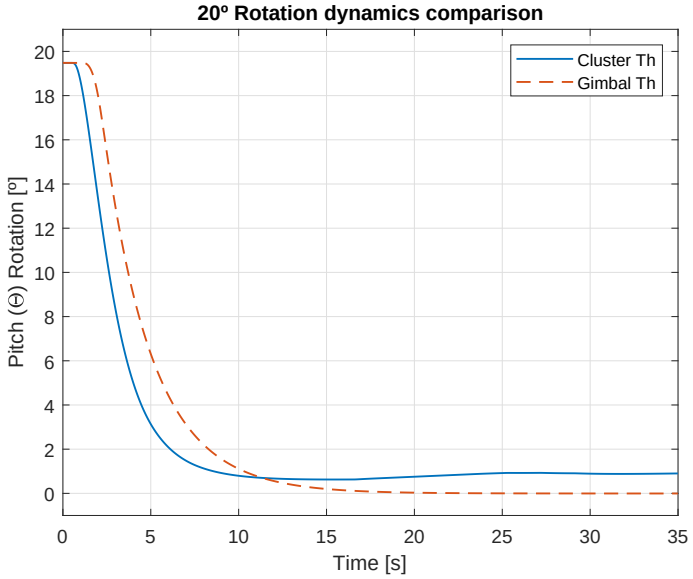

Figure 21: Comparison between configurations in a 20^o turn.

Now, if we take a look at landing safety criteria (*Fig.22*), we can see that all the computed simulations safely landed. Indeed this was one of the parameters to design the control. Regarding soft landing velocity, we can see that the gimbaled thruster has usually higher values, this is just result of the constants used for PD. For LQR we computed the optimal control for multiple points in between the maximum and minimum mass (more than 500) and that might explain the variation on the landing velocity and maximum acceleration.

Regarding the maximum acceleration chart, we can see that for lower masses the maximum acceleration is bigger and its peak is at 6 G's. This isn't a big problem because of 2 reasons:

- Pilots are prepared to tolerate high accelerations for up to 10 seconds or more [8], and in this case the maximum acceleration is when touching the ground, and lasts milliseconds. We

should be careful because this is safety criteria but it doesn't seem as a great problem in this case.

- Small landers (Biggest G force) can't have humans as payload and most of electronic devices aren't as sensitive to big accelerations.

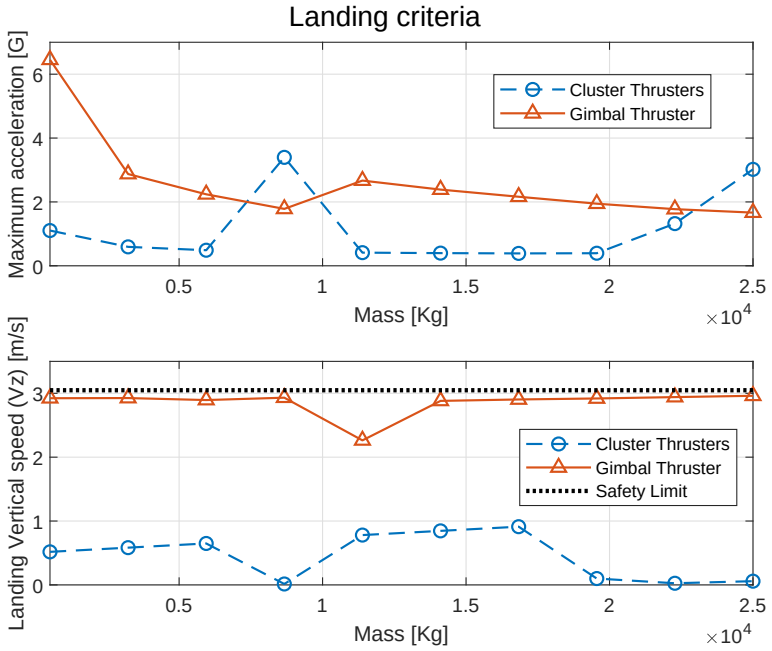

Figure 22: Landing Criteria Check. (a) Maximum Acceleration , (b) Soft landing Velocity

5.2 Fuel consumption

For this section, we show the computed consumption to analyse it's relation with the mass of the lander. To make an non-dimensional parameter (to be able to compare), we calculated it as the weight consumed divided by the total weight, this is:

$$\%ConsumedFuel = \frac{M_0 - M_f}{M_0} * 100$$

- Where M_0 and M_f are initial and final masses of the Lander.

In the graph (Fig.23) we can see a descent trending line for both configurations. This is because the bigger is the engine, the better thrust to weight ratio has, thus the engine is more efficient. This also can explain the lower consumption of the one thruster configuration, and this is what logic suggests. However, as stated before, due to the different controllers used it isn't a very accurate comparison. The first point of the data was taken out of the trending line because it's obviously not representative of the global trend.

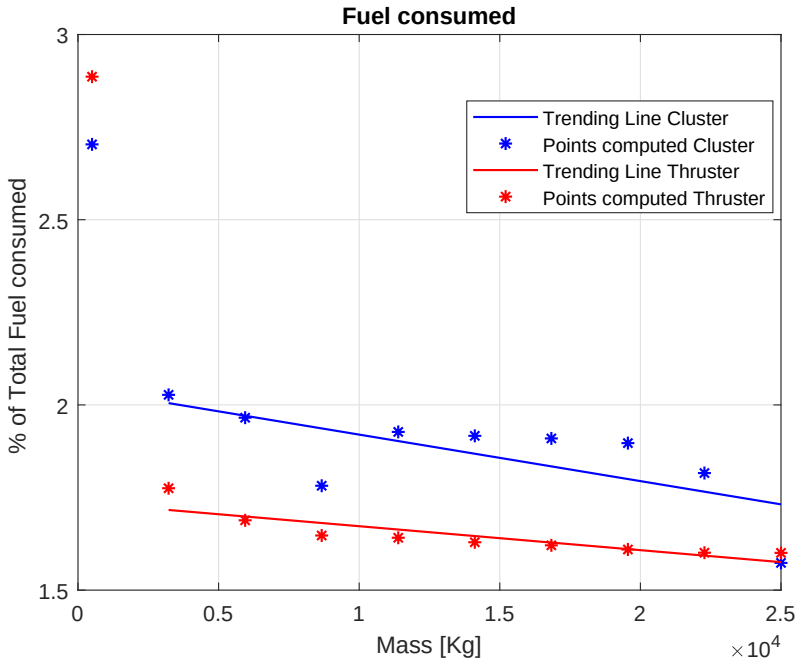

Figure 23: Fuel consumption for objective masses. **Note: The first point is out of the trending line because it's to far from others.*

5.3 Applications

The idea of this section is to analyse the research and results to try to draft the most convenient choice of configuration, depending on the requirements of the mission. Following a lander classification from less mass to more:

1. **Landing missions**
   The main goals of this kind of landers is just prove the feasibility of landing on a planetary body, and gather some useful information (pictures, surface and environmental data...). These don't require big masses, thus the election on the engine configuration isn't that critical, because the weight saving is not as big as for big landers. Furthermore, the additional dry weight of the actuators for the gimbaled configuration doesn't compensate this saving on engines election.

   In this case the cluster of thrusters is more than an acceptable option, depending on the number and disposition, they can increase the safety on landing if one of them can't be used (The other ones can handle the terminal phase). Besides, the fast response characterizing this configuration can help avoiding space debris or other possible inconveniences during the mission. As we have said, the fuel consumption in relative values can be more than the gimbaled thruster, but in absolute values the difference isn't that big, and is compensated by the need of actuators on gimbaled thrusters. Always having in mind that sending one extra kg of payload with the space company Astrobotic to the moon costs around 1.2 million$. Astrobotic themselves use the cluster configuration.

2. **Rover and sample return**
   For this kind of missions the total weight is bigger, because the addition of a rover and the requirement of returning to the earth increases the fuel mass and systems needed to perform the mission. Thus the structure has to be even more heavy to withstand the stresses.

   Another thing to take into account is the size considerations. The diameter of the lander is critical for the effectiveness of the cluster to cause a change of rotation attitude (cause a rotation torque) . Hence, we can assure that the further the engines are, the better, but this brings with it an intrinsic disadvantage, the fuel and electronic systems have longer distance to cover (more dry weight for the same thruster). Also, the lander has to fit in the launcher rocket, limiting geometry. That added to the fact that bigger engines have better thrust to weight ratio, makes gimbaled option more desirable. However, for this cases it's difficult to say which configuration is better, depends on other design choices.

3. **Crewed missions**
   The need of life support systems and space for the crew, increases the mass requirements. Hence, the importance of thrust to weight ratio on engines increases. However, the size and mass of the actuators don't variate that much which could be a big way of reducing costs.

   Besides, for big landers there is an additional problem with cluster configurations. The bigger are the engines the harder is to dissipate the heat created by the engines, which

could cause problems for long burns. Finally, from a fluid mechanics point of view, the cluster configuration creates interaction between exhaust jets (high under-expanded jets, as the moon has very low density atmosphere) which can create undesired lateral forces also. Thus, for this kind of landers, the heaviest ones, the most interesting TVC configuration is the gimbaled thruster. Indeed, the Apollo program had this configuration.

6 Conclusions and remarks

This section, divided in two, will set the conclusions of the thesis and the ways that future students can improve the model.

6.1 Conclusions

In this thesis we have accomplished the goals of researching previous landers, and developing a first model applicable for each mass configuration, taking into account: different engines, geometry definition, inertia matrices, fuel consumption...

However, due to the ambition of the initial idea, and the limited time, some of the more sophisticated ideas (better control, detailed model of the actuators...) have been left to future students.

To sum up, the in-depth research about the history of the Landers and its configurations as well as the engines, gives us a good model base to improve in future versions. Furthermore, despite the assumptions taken, some relevant ideas had come out, such as the importance of the control and the dynamic behaviour of landers.

6.2 Future model development

The main areas in which i think it would be interesting a further development are:

1. Control and trajectory of the Lander: Use optimal configurations for both cases
2. Better model for the actuators: to accurately compute the stresses handled
3. Engine model: to compute accurately fuel's consumption.
4. Thermodynamics approach
5. Landing structural frame : to compute properly the soft landing phase
6. Surface of the planet model : Model of the lunar soil and topology.

**The code is at [12] and [11] online.*

References

[1] NASA, *Apollo Lunar Module News Reference, Grumman Aircraft Engineering Corporation* 1968

[2] CSM/LM, *Spacecraft Operational Data Book, Volume 3, Mass Properties,* SNA-8-D-027(III) Rev 2, 20 August 1969

[3] Sci China Tech Sci, *Sun Z Z, Jia Y, Zhang H. Technological advancements and promotion roles of Chang'e-3 lunar probe mission. 2013, 56:27022708, doi: 10.1007/s11431-013-5377-0*

[4] European Space Agency, *https://spaceflightnow.com/news/n1211/20moonlander/#.UKz1ZuS5OM4*

[5] Aerojet Rocketdyne, *http://www.rocket.com/common-extensible-cryogenic-engine*

[6] DELFT, *Modern Liquid Propellant Rocket Engines, 2000 Outlook, By B.T.C. Zandbergen*

[7] NASA, *STUDY OF POWERED-DESCENT TRAJECTORIES FOR MANNED LUNAR LANDINGS by Floyd V. Bennett and Thomas G. Price, Manned Spacecraft Center Houston, Tex.* AUGUST 1964

[8] NASA/SP-2013-605, *An Analysis and a Historical Review of the Apollo Program Lunar Module Touchdown Dynamics. George A. Zupp, PhD Engineering Directorate, Retired Structural Engineering Division NASA Johnson Space Center, Houston, TX 77058*

[9] Université Catholique de Louvain, *Docquier N., Poncelet A., and Fisette P.: ROBOTRAN: a powerful symbolic generator of multibody models, Mech. Sci., 4, 199-219, doi:10.5194/ms-4-199-2013, 2013.*

[10] NASA, *https://www.nasa.gov (Excerpt from Basics of Space Flight)*

[11] Gimbaled Thruster Code, *https://github.com/curts20/Master-thesis-Gimbaled-thruster.git*

[12] Cluster Thruster Code, *https://github.com/curts20/Master-thesis-uclouvain.git*

A Appendix: Apollo Mass and geometry

Extracted form [1] and [2]

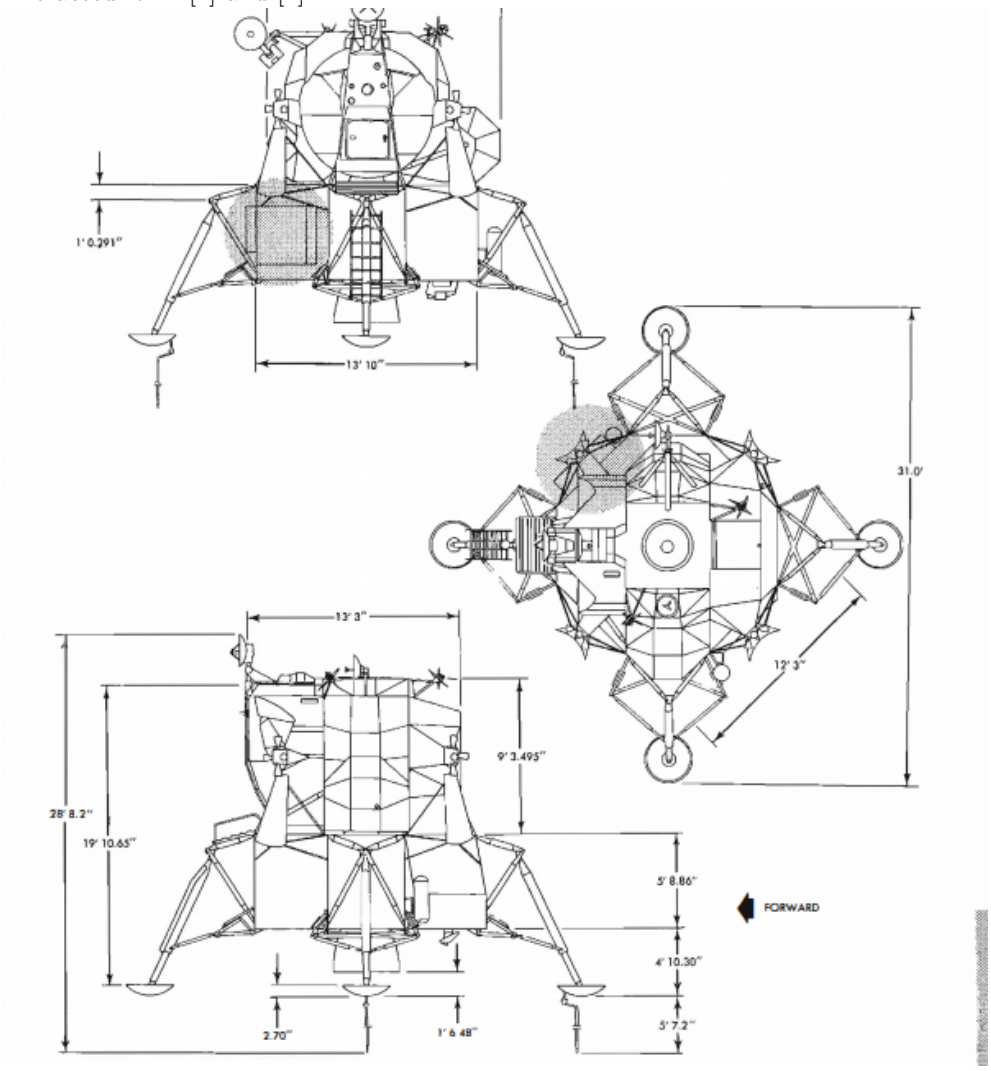

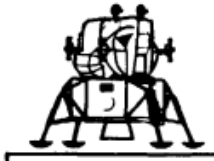

XE COORDINATES

TABLE 3.1-1
LM-10 EXPECTED SEQUENTIAL MASS PROPERTIES

DESCRIPTION	S	WEIGHT POUNDS	C.G. INCHES			INERTIAS SLUG-FT2			PRODUCTS SLUG-FT2			DISPERSIONS LB/IN			
			X	Y	Z	IXX	IYY	IZZ	PXY	PXZ	PYZ	DW	DX	DY	DZ
ASCENT STAGE	+	4799.3	257.9	-.3	2.8	2760	2669	1570	61	111	-18	25.0	.0	.5	.5
39 LM RCS FUEL	+	102.9	279.1	49.6	14.5	0	0	0	0	0	0	1.0	.0	.1	.1
37 LM RCS FUEL	+	102.9	279.1	-49.6	-14.5	0	0	0	0	0	0	1.0	.0	.1	.1
28 LM RCS OXY	+	200.3	275.9	49.6	14.5	0	1	1	0	0	0	2.0	.0	.1	.1
31 LM RCS OXY	+	200.3	275.9	49.6	-14.5	0	1	1	0	0	0	2.0	.0	.1	.1
22 LM APS FUEL	+	2005.5	228.0	-71.3	.0	0	0	0	0	0	0	8.9	.0	.5	.5
19 LM APS OXY	+	3217.3	228.0	49.5	.0	0	0	0	0	0	0	8.7	.0	.5	.5
ASCENT STAGE		10572.5	249.0	-.1	1.3	6627	3317	6022	57	150	-96	27.2	.6	.3	.3
DESCENT STAGE	+	6180.0	156.9	2.6	-7.7	6885	9825	3750	139	-91	262	25.0	.0	.5	.5
77 LM DPS FUEL	+	3755.1	160.9	54.0	.0	0	7	7	0	0	0	7.1	.0	.5	.5
80 LM DPS FUEL	+	3755.1	160.9	-54.0	.0	0	7	7	0	0	0	7.1	.0	.5	.5
71 LM DPS OXY	+	5987.5	160.9	.0	54.0	0	13	13	0	0	0	12.7	.0	.5	.5
74 LM DPS OXY	+	5987.5	160.9	.0	-54.0	0	13	13	0	0	0	12.7	.0	.5	.5
DESCENT STAGE		25665.2	159.9	.6	-1.8	19215	12981	8593	129	-60	292	32.9	.5	.2	.2
LM AT EARTH LAUNCH		36237.7	189.1	.9	-.9	25859	27369	24117	87	515	192	92.3	.9	.2	.2

UNIVERSITÉ CATHOLIQUE DE LOUVAIN
École polytechnique de Louvain
Rue Archimède, 1 bte L6.11.01, 1348 Louvain-la-Neuve, Belgique | **www.uclouvain.be/epl**